Quasiclassical-trajectory Monte Carlo methods for collisions with two-electron atoms

James S. Cohen
Theoretical Division, Los Alamos National Laboratory, Los Alamos, New Mexico 87545
(Received 14 February 1996)

A quasiclassical-trajectory Monte Carlo (QTMC-EB) model is proposed to extend the classical-trajectory Monte Carlo (CTMC) method to targets having more than one electron. Quasiclassical stability is achieved via constraining potentials that enforce lower *energy bounds* on the one-electron dynamics. Cross sections for all possible electronic rearrangements (single and double electron transfer, single and double ionization, and transfer ionization) in $H^+ + H$, $H^+ + He$, $He^{2+} + He$, and $Li^{3+} + He$ collisions are calculated with this model and with the previously proposed model (QTMC-KW) of Kirschbaum and Wilets [Phys. Rev. A **21**, 834 (1980)]. The results are compared with accurate experimental data. The regime of validity for the two-electron targets is found to be similar to that of the usual CTMC model for one-electron targets. [S1050-2947(96)05607-7]

PACS number(s): 34.10.+x, 34.70.+e, 34.50.Fa, 03.65.Sq

I. INTRODUCTION

Since being introduced by Abrines and Percival [1], the classical-trajectory Monte Carlo (CTMC) method has enjoyed numerous successes where quantum-mechanical methods are difficult to apply. The greatest use has been for ion-atom collisions [2] at intermediate energies ($v \sim 1$ a.u.). Here quantum-mechanical close-coupling calculations are limited in practice by basis-set incompleteness and are complicated by translational factors if electronic momentum is to be conserved. The CTMC method has also been useful for collisions of heavy negative particles (e.g., μ^- or $\overline{p}$) with atoms [3], even at low energies ($v \ll 1$ a.u.), where electronic continua are crucial. Time-dependent quantal methods [4,5] can in principle treat both types of problems, but they have not yet proved capable of providing the numerous cross sections that are required in many applications. Such methods are limited by finite-boundary conditions, and the most used method of this type — time-dependent Hartree-Fock (TDHF) theory — neglects correlation, which turns out to be essential in exotic atom formation [6,7].

The CTMC description[1] is rigorously justified by the correspondence principle for reactions of high Rydberg orbitals [1,9], but has been demonstrated by years of experience to be practically accurate for many applications to ground and low excited states as well [2]. This success may be partially attributed to precise obedience of all conservation laws and treating the dynamics, albeit classical, exactly.

Thus far, this advantage has generally been limited to one-electron systems since multielectron atoms are classically unstable with respect to autoionization. Some useful calculations have been managed on multielectron systems by invoking additional approximations such as (i) treating the atom as a one-electron system with an effective charge [10] or a model potential [11], and sometimes expressing the multielectron cross sections as combinations of probabilities from single-electron atoms (the independent-electron model) [12,13], (ii) choosing special initial conditions like the Bohr model of the helium atom and looking at fast collisions only at short times before autoionization can occur [14], or (iii) neglecting the electron-electron interactions that allow autoionization [15,16].

A bold different approach was proposed by Kirschbaum and Wilets (KW) [17]. They added effective potentials, V_H and V_P, motivated by the Heisenberg and Pauli principles, to the pure Coulomb interparticle potentials describing the atom. These potentials (applied to $r_i \times p_i$ with respect to the nucleus for V_H and to $r_{ij} \times p_{ij}$ between electrons i and j for V_P) serve to prevent classical collapse by excluding the electrons from quantum-mechanically forbidden regions of phase space. The resulting quasiclassical states cannot autoionize, and the stability does not depend on any special configuration of coordinates and momenta. A remarkable feature of this approach is that ground-state energies can be obtained by minimizing the energy functional corresponding to the effective Hamiltonian. It has been shown that this simple *ansatz* determines total energies for all atoms with surprising accuracy [18]. The resulting atoms exhibit a shell structure though it is not always in agreement with the structure of the actual atoms. A discomforting feature is that these ground states are ''crystalline;'' i.e. the velocities $\mathbf{v}_{\mathrm{KW}} = d\mathbf{r}_{\mathrm{KW}}/dt$ in the ground state are zero though the momenta are not (so $\mathbf{p}_{\mathrm{KW}} \neq m\mathbf{v}_{\mathrm{KW}}$).

The success of the QTMC-KW model[2] for atomic structure is encouraging, but it is for collisions where such a method is practically needed. In particular, it is desirable to have a method that consistently treats electron transfer and ionization as well as multiplicities and combinations of these processes. Such a unified treatment is easily provided by solution of classical equations of motion and will be useful provided the effective Hamiltonian realistically represents the requisite physical forces at work. Here we may have some concern about the QTMC-KW model. For example, it

[1]The CTMC method has also been much used for rotationally inelastic atom-molecule collisions on adiabatic potential surfaces. Quantum-mechanical calculations, e.g., Vesovic *et al.* [8] recently, have confirmed the accuracy of those cross sections.

[2](Quasi)classical-trajectory Monte Carlo methods belong to a class referred to as ''molecular dynamics,'' and QTMC-KW is sometimes called ''Fermi molecular dynamics.''

is well known that velocity matching can play an important role in electron-transfer processes [19], but a ground-state KW target has no internal motion. This feature is not necessarily fatal since $p_{\mathrm{KW}} \neq m v_{\mathrm{KW}}$, but needs careful investigation. Another concern is that the constraint potential is still significant in a target ground state [18] (e.g., $V_H = 0.09 E_{\mathrm{tot}}$ for He). Of course, it has to be significantly repulsive to prevent access to quantum-mechanically forbidden regions, but its effect on particle motions in allowed regions also needs to be investigated.

Until now the QTMC-KW method has not been carefully tested for collisions, though one limited application was very encouraging [20]. The method has also been applied to multielectron atoms in strong fields [21,22] and to formation of antiprotonic helium [23].

The objectives of the present work are twofold: (i) apply QTMC-KW to diverse cross sections that are now known accurately from experiments and (ii) present a model that avoids the concerns mentioned in the above paragraph. Our model is not as ambitious as the KW model in that it makes no attempt to determine ground-state energies independently. However, it is closer in spirit to the original CTMC method of Abrines and Percival [1], which was to do purely classical mechanics on a microcanonical ensemble of target atoms (i.e., a random phase-space distribution on the energy shell of the actual quantum-mechanical atom). There is no constraint other than energy on the initial condition. For the H atom in CTMC with a pure Coulomb potential, this distribution can be achieved by a simple sampling of certain statistically independent and uniformly distributed variables [1,9,24]. For multielectron and non-Coulomb atoms, such a choice of analytic variables is not known, but the sampling is still easily achieved on a computer by choosing all the phase-space variables at random and *then* testing to see if they yield an energy on (or sufficiently close to) the energy shell of the entire atom. But this is a straightforward numerical problem; the fundamental problem is stability.

In the proposed method, stability is enforced by a constraint on the energies instead of the phase-space variables. Other electrons are not allowed to become so bound that some electron can gain escape energy. The lower bound is imposed on the one-electron energies and is significantly lower than the average electron energy, so that the effective potential implementing it affects the electron motions only when they try to venture into an autoionizing configuration. Hence for the *isolated* hydrogen atom, with only one electron, the motion is never affected and the velocity of the electron is the same as in CTMC. The new method will be termed QTMC-EB for energy-bounded QTMC.

The present applications will be limited to two-electron targets (and $p+\mathrm{H}$ collisions, which apparently have not been published previously for the QTMC-KW model). Fortunately there exist benchmark experimental data for H^+, He^{2+}, and Li^{3+} collisions with He resulting in single and double electron transfer, single and double ionization, and transfer ionization.

II. QUASICLASSICAL-TRAJECTORY MONTE CARLO (QTMC) METHODS FOR MULTIELECTRON TARGETS

The formulation of the quasiclassical Hamiltonians and the initial ground-state configurations will be described in Secs. II A and II B, respectively. The formulation and numerical solution of the equations of motion and the extraction of final states are the same in either case and will be discussed in Sec. II C.

A. Kirschbaum-Wilets (KW) approach

Our QTMC-KW application follows the original prescription of Kirschbaum and Wilets [17]. The associated quasiclassical Hamiltonian adds constraining potentials, V_H and V_P, motivated by the Heisenberg and Pauli principles, to the actual physical Hamiltonian H_0. Thus

$$H_{\mathrm{KW}} = H_0 + V_H + V_P \tag{1}$$

where

$$H_0 = T + V_{\mathrm{Coul}}. \tag{2}$$

For an atom(or ion)-atom collision, in space-fixed coordinates for simplicity, the kinetic energy, as usual, is

$$T = \frac{p_a^2}{2m_a} + \frac{p_b^2}{2m_b} + \frac{1}{2m_e}\sum_i p_i^2, \tag{3}$$

where a and b denote the nuclei and the i index the N_a electrons of atom A and N_b electrons of atom B. The Coulomb potential is

$$V_{\mathrm{Coul}} = \frac{Z_a Z_b e^2}{r_{ab}} - \sum_{\gamma=a}^{b}\sum_{i=1}^{N_a+N_b}\frac{Z_\gamma e^2}{r_{\gamma i}} + \frac{1}{2}\sum_{\substack{i,j \\ (i\neq j)}}\frac{e^2}{r_{ij}}, \tag{4}$$

where $\mathbf{r}_{\alpha\beta} = \mathbf{r}_\beta - \mathbf{r}_\alpha$ $(\alpha,\beta = a,b,1,2,\ldots)$. The extra terms, representing nonclassical constraints, are

$$V_H = \sum_{\gamma=a}^{b}\sum_{i=1}^{N_a+N_b} v_H(r_{\gamma i}, p_{\gamma i}) \tag{5}$$

and

$$V_P = \frac{1}{2}\sum_{\substack{i=1 \\ (i\neq j)}}^{N_a+N_b}\sum_{j=1}^{N_a+N_b}\delta_{s_i,s_j} v_P(r_{ij}, p_{ij}), \tag{6}$$

where the relative momenta are

$$\mathbf{p}_{\alpha\beta} = \frac{m_\alpha \mathbf{p}_\beta - m_\beta \mathbf{p}_\alpha}{m_\alpha + m_\beta} \tag{7}$$

and $\delta_{s_i,s_j} = 1$ if the spins of the ith and jth electrons are the same and 0 if they are different. The constraining potentials are chosen of the form

$$v_c(r,p) = \frac{(\xi_c \hbar)^2}{4\alpha_c r^2 m}\exp\left\{\alpha_c\left[1 - \left(\frac{rp}{\xi_c\hbar}\right)^4\right]\right\} \tag{8}$$

$(c = H \text{ or } P)$, where m is the reduced mass and α_c is a hardness parameter determining how abruptly the constraint $rp \geqslant \xi_c \hbar$ is enforced.[3] Note that asymptotically $(r_{ab} \to \infty)$

[3]The prefactor in Eq. (8) is chosen such that $(\partial/\partial p)[(p^2/2m) + v_c(r,p)] = 0$ for the pair of particles when $rp = \xi_c \hbar$ [25].

H_{KW} is invariant under separate rigid-body rotations of the $\mathbf{r}_{\gamma i}$ and $\mathbf{p}_{\gamma i}$ with respect to nucleus γ. We have neglected the spin of the nuclei and its possible effect in the case of identical nuclei.

The energy functional (1) can be minimized to determine ground-state energies. This was done in Ref. [18] for atoms and ions up to $Z=38$. By using the scaled value

$$\xi_c=\xi_c^{\infty}\left(1+\frac{1}{2\alpha_c}\right)^{-1/2}, \tag{9}$$

where $\xi_H^{\infty}=1.0$ and $\xi_P^{\infty}=2.767$, it was found that the energies depend only weakly on the hardness parameter α_c as long as it is not too small. Hence the choice of α_c is based largely on numerical considerations and the physical information resides mostly in the ξ_c's. In the present work $\alpha_c=4$ was used (except for sensitivity studies). This value is slightly smaller than the value $\alpha_c=5$, used in Ref. [18], but makes the numerical integration a little easier.

It is possible to take different values of ξ_H for each nucleus. For processes involving only one transferred electron, this flexibility may enable better results; however, for processes involving more electrons it might be considered inconsistent since it could result in different treatments of isoelectronic systems. This effect will be examined in Sec. III B.

The KW ground state is described by fixed values of $\mathbf{r}$ and $\mathbf{p}$. It is invariant under independent rigid-body rotations but is otherwise thought to be nondegenerate. Following the original prescription of Abrines and Percival [1], we always assume that, once the Hamiltonian has been defined, the microcanonical distribution (random in phase space on the energy shell) is the appropriate physical choice [9]. There are compelling physical reasons for this choice, especially if the motion is ergodic, and it avoids any bias. Thus the correct Monte Carlo sampling of KW initial conditions is obtained by performing random Euler rotations of any ground-state configuration. In general, numerical minimization [18] is required to find the ground-state configuration and energy, but the one- and two-electron cases can be solved analytically [17]. For the one-electron atom

$$r_{\gamma 1}^{(0)}=\left(1+\frac{1}{2\alpha_H}\right)\frac{[\xi_H(\gamma)]^2}{Z_\gamma} \tag{10a}$$

and

$$p_{\gamma 1}^{(0)}=\xi_H(\gamma)/r_{\gamma 1}^{(0)}. \tag{10b}$$

For the two-electron atom

$$r_{\gamma 1}^{(0)}=\left(1+\frac{1}{2\alpha_H}\right)\frac{4[\xi_H(\gamma)]^2}{4Z_\gamma-1}, \tag{11a}$$

$$\mathbf{r}_{\gamma 2}^{(0)}=-\mathbf{r}_{\gamma 1}^{(0)}, \tag{11b}$$

$$p_{\gamma 1}^{(0)}=\xi_H(\gamma)/r_{\gamma 1}^{(0)}, \tag{11c}$$

and

$$\mathbf{p}_{\gamma 2}^{(0)}=-\mathbf{p}_{\gamma 1}^{(0)}. \tag{11d}$$

B. Energy-bounded (EB) approach

In the QTMC-EB approach, the quasiclassical potential includes terms placing lower bounds on the one-electron energies ignoring all other electrons. The bounds are low enough that the electron motions in the ground state are little affected, but high enough that autoionization is precluded. As in the KW approach, the bound is introduced numerically with a repulsive potential.

This quasiclassical Hamiltonian for an atom(ion)-atom collision is

$$H_{\mathrm{eb}}=H_0+V_{\mathrm{eb}}, \tag{12}$$

where H_0 is the same as in Eq. (2). The constraint potential is

$$V_{\mathrm{eb}}=\sum_{\gamma=a}^{b}\sum_{i=1}^{N_a+N_b} v_{\mathrm{eb}}^{(\gamma)}(r_{\gamma i},p_{\gamma i}), \tag{13}$$

where

$$v_{\mathrm{eb}}^{(\gamma)}(r,p)=\frac{Z_\gamma e^2}{r}\exp\left(\frac{E_0^{(\gamma)}-E_{\mathrm{Coul}}}{\Gamma}\right). \tag{14}$$

Instead of the constraint being applied to the product rp as in the KW approach it is applied to the one-electron Coulomb energy

$$E_{\mathrm{Coul}}=\frac{1}{2m}p^2-\frac{Z_\gamma e^2}{r}. \tag{15}$$

In the limit $\Gamma\to 0$, this one-electron energy is bounded from below by exactly the constant $E_0^{(\gamma)}$. For finite Γ, the constraint is softened but still provides an absolute lower bound, which in turn, as long as it is not too low, implies absolute stability of the multielectron atom with respect to *autoionization* (of course, collisional or field ionization can still occur). In the same vein it can be seen that, for a one-electron atom bound by energy $0>E_b>E_0$, the constraint will have no effect on the dynamics for sufficiently small Γ. In practice, Γ is chosen reasonably small but not so small as to create problems with the numerical integration.

The constants $E_0^{(\gamma)}$ are different for different nuclear charges Z_γ, but are perhaps best thought of as depending on a *single* parameter characterizing the lowest one-electron energy allowed relative to the actual binding energy. For this purpose it is useful to ask what is the lowest energy, including the constraint but ignoring all other electrons, that an electron can ever reach. The energy including constraint is

$$\begin{aligned}E&=E_{\mathrm{Coul}}+\frac{Z}{r}e^{(E_0-E_{\mathrm{Coul}})/\Gamma}\\&=E_{\mathrm{Coul}}+(\tfrac{1}{2}p^2-E_{\mathrm{Coul}})e^{(E_0-E_{\mathrm{Coul}})/\Gamma}.\end{aligned} \tag{16}$$

Since the term in p^2 is positive definite, the minimum energy possible is

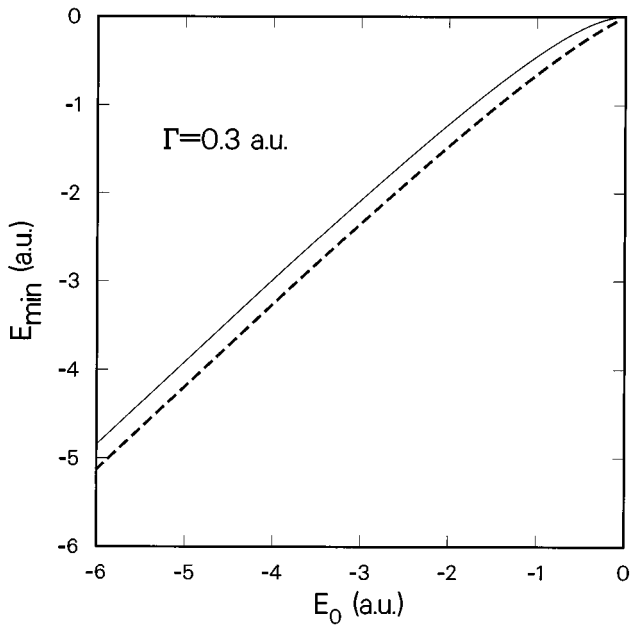

FIG. 1. Minimum energy, $E_{\min}$ (solid curve), reachable in Eq. (16) and the corresponding value of E_{Coul} (dashed curve) as a function of the parameter E_0 for fixed $\Gamma=0.3$ a.u. Note [see Eq. (17)] that the same curves would apply for all Γ if both axes were divided by Γ.

$$E_{\min}=\min\{E_{\mathrm{Coul}}(1-e^{(E_0-E_{\mathrm{Coul}})/\Gamma})\}, \tag{17}$$

where we now regard E_{Coul} as a variable that can take any value. Figure 1 shows the value of $E_{\min}$, along with the value of E_{Coul} when it is achieved, as a function of E_0. This figure is drawn for $\Gamma=0.3$ a.u., but it is obvious from Eq. (17) that the same curves would apply if $E_{\min}/\Gamma$ and E_{Coul}/Γ were plotted as a function of E_0/Γ.

For the present work we have found it satisfactory to choose E_0 such that the lowest one-electron energy allowed classically is ~ 0.5 a.u. lower than the quantum-mechanical ground state of the one-electron system. Specifically we use $E_0(\mathrm{H})=-2.0$ a.u., $E_0(\mathrm{He})=-3.4$ a.u., and $E_0(\mathrm{Li})=-6.1$ a.u., with $\Gamma=0.3$ a.u. in all cases. These choices yield $E_{\min}(\mathrm{H})=-1.22$ a.u., $E_{\min}(\mathrm{He})=-2.44$ a.u., and $E_{\min}(\mathrm{H})=-4.94$ a.u., which are 0.72, 0.44, and 0.44 a.u. lower than the true binding energies of H, He^+, and Li^{2+}, respectively. The sensitivity to these choices will be examined in Sec. III B. The parameter Γ, like α_c in the KW formulation, is chosen largely from consideration of the ease of numerical integration, and E_0, like ξ in the KW formulation, is modified to compensate for its finite value.

Sampling the microcanonical ensemble to find initial conditions requires more effort than in the KW case. Even for the one-electron system it is necessary to do the sampling by trial and error (though we do not claim to have proved that analytic procedures do not exist for special cases). We used the numerical procedure described in Ref. [26]. Basically it consists of randomly choosing a complete set of variables from a prescribed region of phase space, calculating the resulting energy, and checking to see if it falls within some Gaussian profile about the desired energy. If so, it is accepted and a slight renormalization is applied to make the energy exact; if not, it is rejected. The region of phase space sampled is sufficiently large that it is highly unlikely that a random point outside the region would produce an acceptable energy. For H, the uniformly sampled region (in a.u.) was $r^2\in(0,4)$, $p^2\in(0,16)$ with a width of 0.025 about the target energy of -0.5 a.u. For He, the sampled region was $r^2\in(0,4)$, $p^2\in(0,12.96)$ for each electron with a width of 0.1 about the target energy of -2.9 a.u. The resulting list of initial conditions can be saved for use in all trajectory calculations, but, even so, this procedure might be too time consuming for many-electron targets. It is likely that a more efficient, yet still statistically valid, procedure could be developed.

C. Treatment of the dynamics

This section will be brief since, once the effective Hamiltonian is defined and the initial coordinates and momenta selected, the treatment is the same as in previous CTMC calculations. The calculations proceed in three steps: (i) choose initial conditions, (ii) integrate Hamilton's classical equations of motion, and (iii) test asymptotic trajectory for final state.

The selection of the initial atomic configurations was discussed in Secs. II A. and II B. In addition, an impact parameter must be chosen by uniform sampling of $b^2\in[(b_i^{\min})^2,(b_i^{\max})^2]$. Our procedure was to do the calculation with a few ranges of impact parameter, starting with $b_1^{\min}=0$; typically 3–4 ranges contributed. The number of trajectories in the first range, up to some maximum, was determined by a relative accuracy criterion on the total *reactive* cross section. The number of trajectories, again up to some maximum, in subsequent ranges was determined by the accuracy actually achieved up to that point. This procedure is efficient since usually the reactive probability decreases as b increases, and it will subsequently not be possible to improve the relative accuracy much anyway. The advantages of this procedure over doing all in a single range are that the maximum impact parameter does not have to be chosen in advance and fewer trajectories need be run in the less important regions.

Hamilton's equations were solved in a barycentric coordinate system after eliminating the overall center-of-mass motion. This formulation, which has previously been described in detail for the four-body system [15], eliminates six variables from the set of ordinary differential equations. The price paid is the extra complexity of the resulting coordinates and the necessity of transformations between different barycentric coordinate systems (three for the four-body problem). For more than four bodies it will probably be more practical to integrate the equations in space-fixed coordinates.

The ODE's were integrated with the same subroutine used in all our previous CTMC work [3] (sixth-order hybrid method of Gear). There may well exist more suitable integrators for this problem. The constrained trajectories, of either the KW or EB variety, are somewhat more difficult to integrate than pure Coulomb classical trajectories. The integration is made more difficult for large α_c (in QTMC-KW) or small Γ (in QTMC-EB). The automatic time step tends to become small in highly constrained regions and was not allowed to fall below some specified minimum value. None-

theless the integrator failed very rarely, and all conservation laws, including energy and angular momentum, were generally fulfilled quite accurately. Still more demanding tests, made occasionally, indicated that most of the trajectories could be back-integrated with meaningful accuracy.

The trajectories were integrated long enough that the final state could be definitely identified by checks on relative distances, relative velocities, and internal and relative energies [3]. After accumulation of the results of the trajectories, the cross section for a reaction R is given by

$$\sigma_R = \sum_i \sigma_R^{(i)} \tag{18}$$

in terms of the partial cross sections

$$\sigma_R^{(i)} = \frac{N_i^{(R)}}{N_i^{\rm tot}} \pi [(b_i^{\rm max})^2 - (b_i^{\rm min})^2], \tag{19}$$

where $N_i^{(R)}$ is the number of trajectories in which R occurred out of the total $N_i^{\rm tot}$ trajectories run with $b \in [b_i^{\rm min}, b_i^{\rm max}]$. The standard statistical error in σ_R is

$$\Delta\sigma_R = \left(\sum_i (\Delta\sigma_R^{(i)})^2 \right)^{1/2} \tag{20}$$

in terms of the error in each interval,

$$\Delta\sigma_R^{(i)} = \sigma_R^{(i)} \left(\frac{N_i^{\rm tot} - N_i^{(R)}}{N_i^{\rm tot} N_i^{(R)}} \right)^{1/2} . \tag{21}$$

The total number of trajectories, $N_{\rm tot} = \Sigma_i N_i^{\rm tot}$, varied from about 500 to 5000 for collisions with the helium atom (even more were used for $H^+ + H$ collisions).

III. RESULTS

Cross sections have been calculated for all electron rearrangements occurring in collisions of H^+, He^{2+}, and Li^{3+} ions with the helium atom, as well as for the $H^+ + H$ collision to compare with normal (unconstrained) CTMC. In comparing the Monte Carlo results with each other and with experimental results, it is important to take into account the statistical error bars. The quoted error bars are one standard deviation; differences and anomalies amounting to less than two standard deviations should generally be disregarded. In some cases where such deviations appeared, additional trajectories were run to improve the statistics and allow conclusions to be reached.

For collisions with the helium atom, the QTMC-KW calculations were done two ways: (i) with $\xi(\mathrm{He}) = \xi(\mathrm{H})$ and (ii) with $\xi(\mathrm{He}) = 1.0844\xi(\mathrm{H})$.[4] The latter gives the ionization potentials of both H and He correctly while the former gives IP(He) = 28.9 eV instead of the true value of 24.6 eV. While this alteration may be expected to be beneficial for single ionization, it might be expected to have the opposite effect for double ionization since the effect is to alter the correct second ionization potential of He from the true value of 54.4 eV to 46.3 eV. The modified KW procedure will be designated QTMC-KWx.

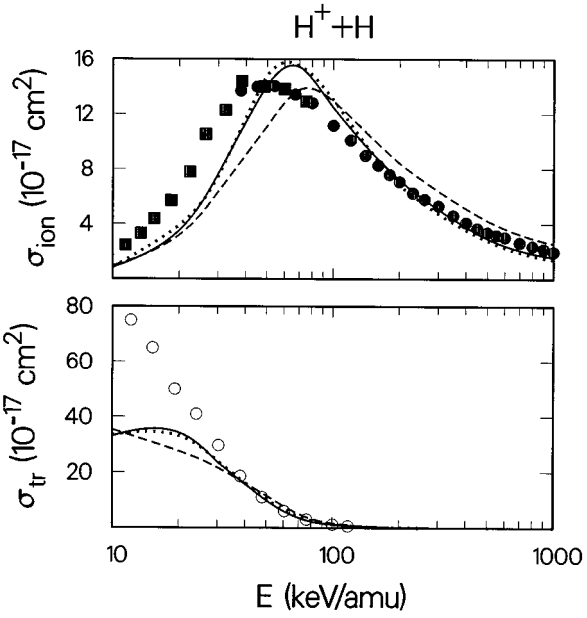

FIG. 2. Electron-transfer and ionization cross sections for $H^+ + H$ collisions. Theoretical values are shown by curves: CTMC (dotted), QTMC-KW (dashed), QTMC-EB (solid). Experimental values are shown by data points: Shah and Gilbody [29] (filled circles), Shah, Eliott, and Gilbody [30] (filled squares), McClure [31] (open circles).

A. $H^+ + H$ collisions

The proton-hydrogen atom reaction was the first treated by electronic CTMC and is still a requisite test case for new methods. However, it seems not to have been presented in published QTMC-KW calculations. The CTMC, QTMC-KW($\alpha = 4$, $\xi = 0.9428$) and QTMC-EB($\Gamma = 0.3$, $E_0(\mathrm{H}) = -2.0$) calculations, along with experimental measurements are shown in Fig. 2 for electron transfer and ionization. A large number of trajectories were run here so the statistical error bars (not shown for clarity) are small.

The CTMC and QTMC-EB results are quite close, thus confirming that the stated philosophy of staying close to purely classical dynamics, even while maintaining quasiclassical stability, has been realized. As a test, calculations were also performed in the limit $E_0 \to -\infty$ (actually -10^6 a.u.) and agreed precisely with CTMC (within statistical error) as they should by construction of the potential. The QTMC-KW results are also similar — the peak in $\sigma_{\rm ion}$ is somewhat shifted to higher energies but is in qualitatively similar agreement with the experimental results.

Kerby *et al.* [27] have interpreted the CTMC underestimation of the ionization cross section at energies below the peak as due to classical suppression of low-energy backward electrons. The rather poor description of electron transfer at low energies is due to inadequate classical description of the symmetric molecular states that serve as intermediaries in this transition.

[4] The subscript H on ξ will be henceforth dropped since only ξ_H is involved in the descriptions of the hydrogen atom or singlet helium atom.

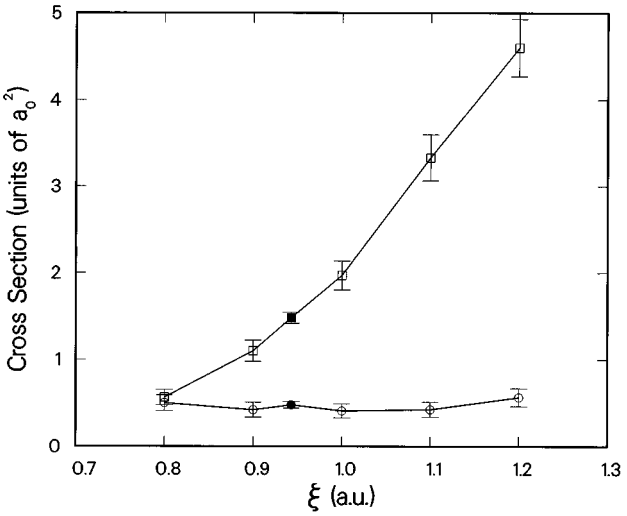

FIG. 3. Sensitivity of the transfer (circles) and ionization (squares) cross sections to the parameter ξ in the QTMC-KW model for $p+$He collisions at proton energy 100 keV. The filled points are at the value of ξ generally used. $\alpha=4$ in these calculations. The error bars indicate one standard deviation of the Monte Carlo calculations. The lines connecting the points are just meant to guide the eye.

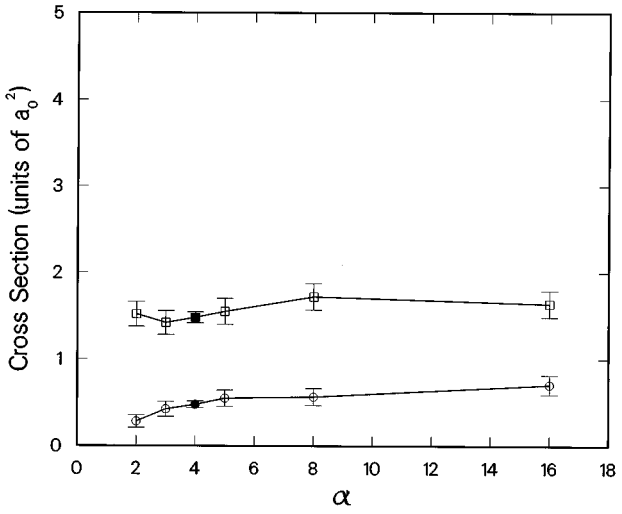

FIG. 4. Sensitivity of the transfer (circles) and ionization (squares) cross sections to the hardness parameter α in the QTMC-KW model for $p+$He collisions at proton energy 100 keV. The filled points are at the value of α generally used. Note that the corresponding value of ξ has been adjusted in each case to give the correct energy of the H atom.

B. Sensitivity studies

In this section the sensitivities of the electron-transfer and ionization cross sections to the parameters of the constraining potentials will be examined. The $H^+ + He$ collision at projectile energy 100 keV ($v=2$ a.u.) will be taken as a typical example.

In Figs. 3 and 4, the sensitivities of the QTMC-KW results to ξ and α, respectively, are shown. It is evident that $\sigma_{\rm ion}$ is quite sensitive to ξ while $\sigma_{\rm tr}$ is not. The sensitivity of $\sigma_{\rm ion}$ is to be expected since the atomic binding energy is inversely proportional to ξ^2 and the size of the atom is proportional to ξ^2. The insensitivity of $\sigma_{\rm tr}$ to ξ is somewhat surprising. In this test the ξ values for both atoms were varied, i.e., ξ(He)$=\xi$(H). In calculations where only ξ(He) was changed (the KWx model — see Sec. II A), $\sigma_{\rm tr}$ was more affected.

The sensitivity to α, shown in Fig. 4, is considerably less. It is important to note that in this calculation the corresponding ξ was simultaneously scaled according to Eq. (9) to maintain the same atomic binding energy and size. These results tend to confirm our interpretation of ξ as a physical parameter and α as a numerical-implementation parameter. The value $\alpha=4$ appears to be a reasonable compromise between numerical good behavior and implementation of the constraint, although $\alpha=3$ or $\alpha=5$ would appear to be quite acceptable as well.

In Figs. 5 and 6 the sensitivities of the QTMC-EB results to its parameters, E_0(He) and Γ, are shown. The effects of E_0 and Γ in the QTMC-EB model are analogous to those of ξ and α, respectively, in the QTMC-KW model (although the units are different). The ionization cross section is fairly sensitive to E_0. The reason for the increase in $\sigma_{\rm ion}$ as E_0(He) becomes more negative can be understood in terms of its effect on the phase-space distribution of the two-electron system. When one electron is allowed to become deeply bound the other electron becomes weakly bound since the total energy is conserved. Such a weakly bound electron is easily ionized. Of course, this amounts to just lifting the constraint; as can be seen from Fig. 1, for E_0(He)$=-3.9$ (and $\Gamma=0.3$) autoionization could occur. Figure 5 suggests that E_0 should be chosen such that the energies of the two electrons in the isolated atom are not allowed to become too different — the sensitivity on this side of the figure is much less.

The sensitivity to Γ, like that to α in the QTMC-KW model, is much weaker. Here it is important to note that the corresponding E_0 has been adjusted so that $E_{\rm min}$ (see Fig. 1)

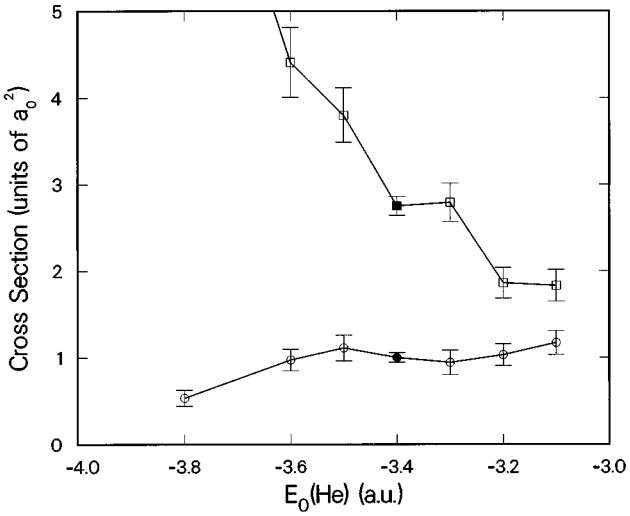

FIG. 5. Sensitivity of the transfer (circles) and ionization (squares) cross sections to the parameter E_0(He) in the QTMC-EB model for $p+$He collisions at proton energy 100 keV. The filled points are at the value of E_0(He) generally used. $\Gamma=0.3$ a.u. was used in all these calculations.

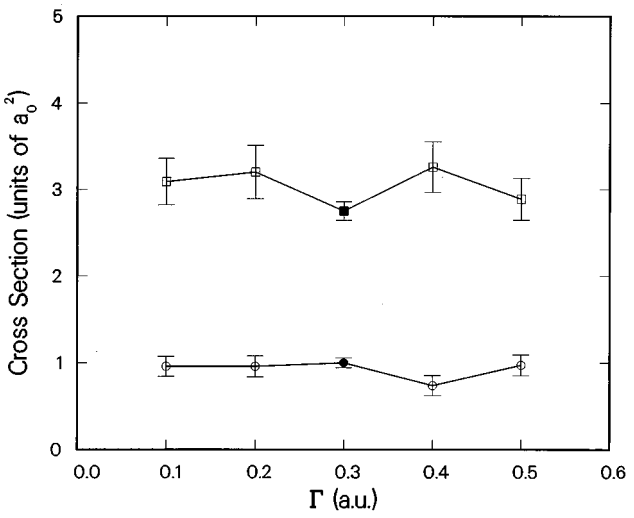

FIG. 6. Sensitivity of the transfer (circles) and ionization (squares) cross sections to the hardness (width) parameter Γ in the QTMC-EB model for $p+$He collisions at proton energy 100 keV. The filled points are at the value of Γ generally used. Note that the corresponding value of E_0(He) has been adjusted in each case to give the same lower bound on the He atom.

is the same for all values of Γ. This is analogous to the adjustment of α discussed above. These results confirm our interpretation of E_0 as a physical parameter and Γ as a numerical-implementation parameter.

Finally we examine the sensitivity to the value of E_0 taken for the projectile ion. The results are shown in Fig. 7

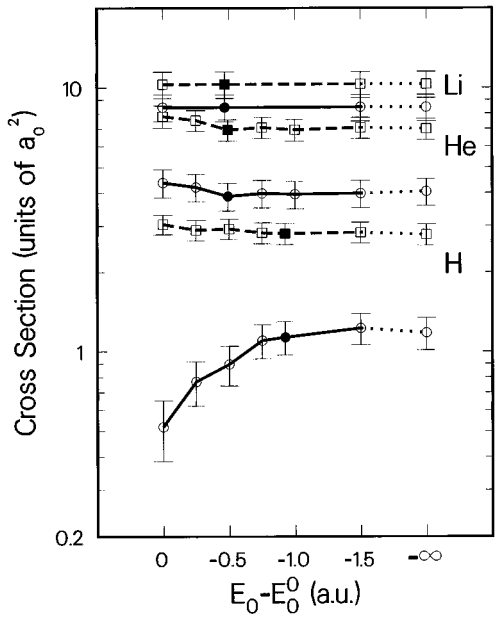

FIG. 7. Sensitivity of the transfer (circles connected by solid curves) and ionization (squares connected by dashed curves) cross sections to the parameter E_0 of the projectile ion in the QTMC-EB model for H^++He, He^{2+}+He, and Li^{3+}+He collisions at projectile energy 100 keV/amu. The E_0 axis has been shifted in each case by E_0^0, the value of E_0 that just allows the ground-state energy of the projectile with one electron to be reached. The filled points are at the values generally used.

for H^++He, He^{2+}+He, and Li^{3+}+He, all for projectile-ion energy of 100 keV/amu. So that the abscissa will be sensibly comparable for all three systems, E_0 has been shifted on the plot by E_0^0, where E_0^0 is the highest value of E_0 that will still allow the transferred electron to reach the ground state on the projectile. Namely, $E_0^0(\mathrm{H})=-1.075$, $E_0^0(\mathrm{He})=-2.909$, and $E_0^0(\mathrm{Li})=-5.631$, which allow minimum energies of -0.5, -2.0, and -4.5 a.u., respectively (see Fig. 1). It can be seen that only the electron-transfer cross section for H^++He collisions is sensitive to the target parameter E_0. This sensitivity arises because the ground-state electrons in H and He have similar velocities and electron-transfer cross sections tend to peak when the velocities match. Classically the ground state is characterized by a range of energies, which must extend somewhat below as well as above the quantized energy [28]. In Sec. III C we will see that the QTMC-KW model underestimates the $H^+ + He \rightarrow H + He^+$ transfer cross section, presumably because lower energies are excluded.

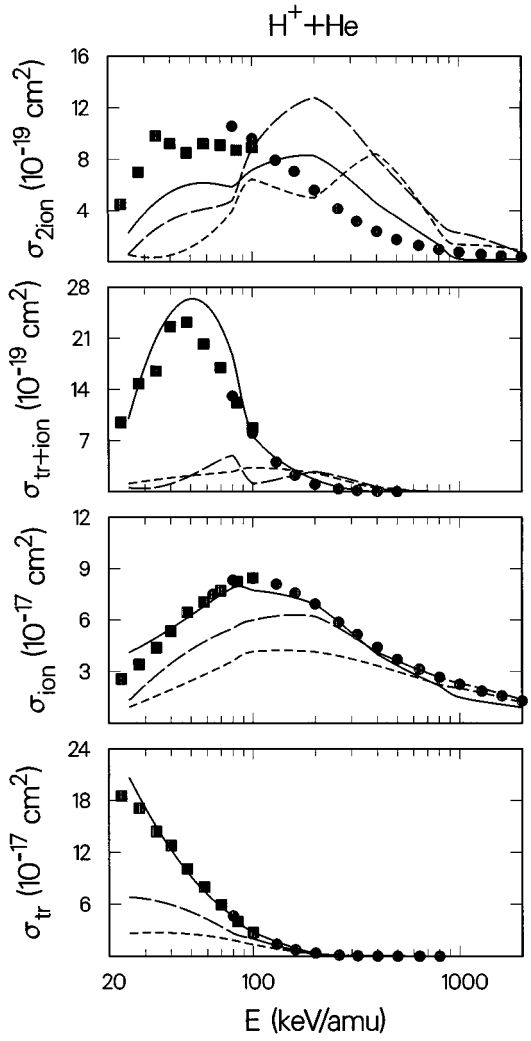

FIG. 8. Cross sections for H^++He collisions. Theoretical values are shown by curves: QTMC-KW (short dashed), QTMC-KWx (long dashed), QTMC-EB (solid). See the tables for the energies at which calculations were actually made and their statistical error bars. Experimental values are shown by data points: Shah and Gilbody [32] (filled circles), Shah, McCallion, and Gilbody [33] (filled squares).

TABLE I. Comparison of cross sections (in units of 10^{-17} cm^2) for the electron-transfer reaction $H^+ + He \rightarrow H + He^+$.

E_p (keV)	v (a.u.)	$_{10}\sigma_{01}$(H,He) Expt [32].	QTMC-KW	QTMC-KWx[a]	QTMC-EB
25.0	1.00		2.64±0.34	6.82±0.66	19.63±1.46
50.0	1.41		2.55±0.32	5.10±0.59	9.19±0.80
80.0	1.79	4.65±0.23	1.85±0.29	2.64±0.35	4.62±0.53
100.0	2.00	2.72±0.10	1.34±0.11	2.02±0.31	2.80±0.16
200.0	2.83	0.365±0.004	0.26±0.11	0.18±0.09	0.31±0.11
400.0	4.00	0.0222±0.0010	0.07±0.03	0.06±0.03	0.06±0.02

[a]With χ(He) modified to give accurate first ionization potential of He.

C. $H^+ + He$ collisions

Cross sections for electron transfer (σ_{tr} or $_{10}\sigma_{01}$), ionization (σ_{ion} or $_{10}\sigma_{11}$), transfer ionization (σ_{tr+ion} or $_{10}\sigma_{02}$), and double ionization (σ_{2ion} or $_{10}\sigma_{12}$) in $H^+ + He$ collisions are shown in Fig. 8 and tabulated including error bars in Tables I–IV. In these calculations the initial internuclear distance was $15a_0$ and the impact parameter ranges (in a_0) were $[0,1]$, $[1,\sqrt{2}]$, $[\sqrt{2},2]$, ... until convergence was obtained. Target relative accuracy was 5% of the total reactive cross section or 200 trajectories per impact-parameter interval, whichever was reached first. In some cases, especially at the higher energies, higher accuracy was sought with larger numbers of trajectories (as can be inferred from the statistical error bars). The double-electron reactions have smaller cross sections and generally occur in collisions at smaller impact parameters. In order to obtain them with better accuracy, additional calculations were made with impact parameter ranges $[0,0.5]$, $[0.5,0.5\sqrt{2}]$, $[0.5\sqrt{2},1]$, ... with the convergence criterion applied only to the double-electron reactions. The trajectories were integrated to a distance — at least $15a_0$ — where the final state could be conclusively identified.

The QTMC-EB method provides a good description of all four $H^+ + He$ cross sections, including the single electron transfer even at the lowest energies treated. The QTMC-KW method does fairly well for ionization but greatly underestimates the transfer reactions. The QTMC-KWx variation of QTMC-KW, in which the ξ(He) parameter has been modified to give the first ionization potential correctly, does better for the one-electron processes, but still underestimates σ_{tr}.

Potentially one of the most useful capabilities of quasiclassical methods may be their ease of treating multielectron rearrangements. The QTMC-EB method gives both the transfer ionization and double ionization cross sections fairly accurately. One may note in the double ionization cross section that there appears to be a ''glitch'' at ~100 keV. This feature occurs in both the experimental and theoretical cross sections. However, the agreement is not really persuasive since there are glitches in other theoretical cross sections that do not show up experimentally.

Energy histograms for the ionized free electron and the residual bound electron after single ionization are shown in Figs. 9(a) and 9(b), respectively, for the QTMC-EB and QTMC-KW calculations. The EB and KW electron-energy distributions are similar, except that the KW peak for the residual He^+ electron at -2.0 a.u. is smeared out in the EB calculation. As usual in quasiclassical calculations, effective quantum numbers have to be assigned to ranges of energies [28].

TABLE II. Comparison of cross sections (in units of 10^{-17} cm^2) for the single-ionization reaction $H^+ + He \rightarrow H^+ + He^+ + e$.

E_p (keV)	v (a.u.)	$_{10}\sigma_{11}$(H,He) Expt. [32]	QTMC-KW	QTMC-KWx	QTMC-EB
25.0	1.00		0.92±0.20	1.32±0.23	4.61±0.73
50.0	1.41		2.46±0.34	4.27±0.46	6.26±0.72
80.0	1.79	8.32±0.13	3.61±0.39	5.50±0.49	7.87±0.73
100.0	2.00	8.43±0.18	4.15±0.18	5.98±0.50	7.72±0.30
200.0	2.83	6.93±0.17	4.13±0.36	6.20±0.48	6.91±0.53
400.0	4.00	4.41±0.09	3.34±0.17	4.12±0.21	4.00±0.21
800.0	5.66	2.67±0.03	2.24±0.14	2.66±0.16	2.17±0.14
1000.0	6.33	2.26±0.08	2.02±0.13	2.32±0.16	1.50±0.12
2000.0	8.95	1.295±0.011	1.21±0.11	1.37±0.12	0.91±0.10

TABLE III. Comparison of cross sections (in units of 10^{-18} cm^2) for the transfer-ionization reaction $H^+ + He \rightarrow H + He^{2+} + e$.

E_p (keV)	v (a.u.)	$_{10}\sigma_{02}$(H,He) Expt. [32]	QTMC-KW	QTMC-KWx	QTMC-EB
25.0	1.00		0.11±0.08	0.05±0.05	1.00±0.27
50.0	1.41		0.22±0.11	0.22±0.11	2.64±0.49
80.0	1.79	1.31±0.08	0.27±0.12	0.49±0.16	2.15±0.35
100.0	2.00	0.80±0.08	0.44±0.15	0.11±0.08	0.77±0.20
200.0	2.83	0.102±0.008	0.22±0.11	0.27±0.12	0.17±0.10
400.0	4.00	0.0071±0.0006	0.04±0.03	0.07±0.04	<0.01[a]

[a]None found in 3000 trajectories.

D. $He^{2+} + He$ collisions

Cross sections for electron transfer (σ_{tr} or $_{20}\sigma_{11}$), ionization (σ_{ion} or $_{20}\sigma_{21}$), transfer ionization (σ_{tr+ion} or $_{20}\sigma_{12}$), double ionization (σ_{2ion} or $_{20}\sigma_{22}$), and double transfer (σ_{2tr} or $_{20}\sigma_{02}$) in $He^{2+} + He$ collisions are shown in Fig. 10 and tabulated in Tables V–IX. The initial conditions were simi-

TABLE IV. Comparison of cross sections (in units of 10^{-19} cm^2) for the double-ionization reaction $H^+ + He \rightarrow H^+ + He^{2+} + 2e$.

E_p (keV)	v (a.u.)	$_{10}\sigma_{12}$(H,He) Expt. [32]	QTMC-KW	QTMC-KWx	QTMC-EB
25.0	1.00		0.55±0.55	0.55±0.55	2.21±1.10
50.0	1.41		1.10±0.78	3.85±1.44	6.05±1.97
80.0	1.79	10.57±1.01	3.96±1.72	4.77±1.99	6.07±1.82
100.0	2.00	9.61±1.03	4.95±1.63	8.80±2.15	7.15±1.97
200.0	2.83	5.60±0.17	3.30±1.34	12.78±3.04	8.27±2.11
400.0	4.00	2.36±0.12	8.43±1.59	8.10±1.60	4.58±1.16
800.0	5.66	0.960±0.051	2.42±0.73	3.08±0.82	1.32±0.54
1000.0	6.33	0.745±0.027	1.32±0.54	2.25±0.71	0.22±0.22
2000.0	8.95	0.365±0.035	0.88±0.44	0.66±0.38	0.22±0.22

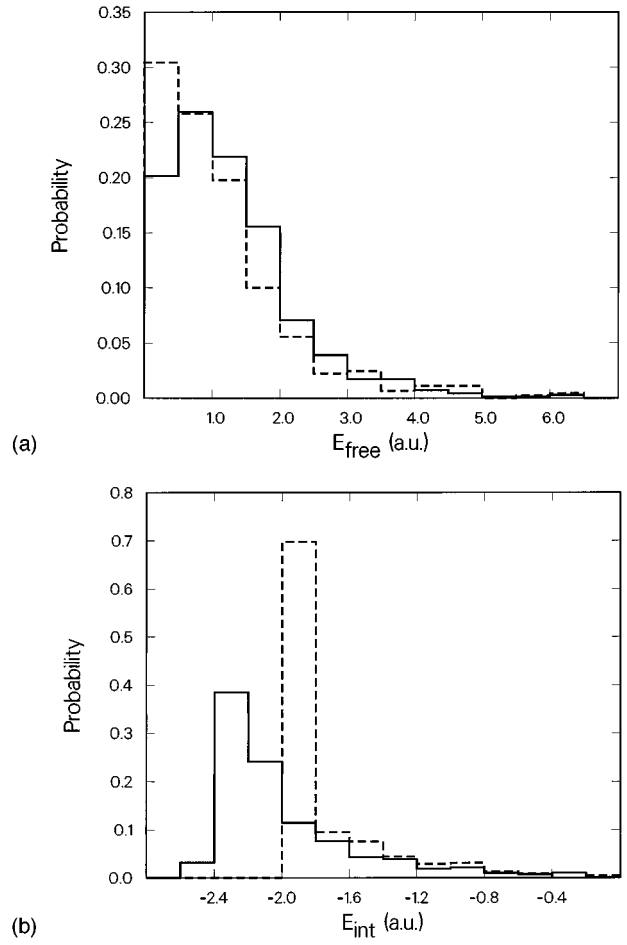

FIG. 9. Histograms of the electron energy distributions of the (a) ionized free electrons and (b) residual bound electrons after single ionization in H^++He collisions at a H^+ energy of 100 keV. The solid curves are the results of QTMC-EB calculations and the dashed curves are the results of QTMC-KW calculations.

lar to those described in Sec. III C except that the initial internuclear distance (and minimum final distance) was 20 a_0 and the first range of impact parameters was [0,1.5] ([0,0.75] for the extra trajectories run for the double electron reactions).

The QTMC-EB results for single and double ionization are good, while those for transfer are not quite as good. The QTMC-KW method seems to get the single transfer cross section precisely while the QTMC-EB cross section is too large at the lower energies. For the double ionization process, the QTMC-EB method appears to be best at energies higher than the peak, while the QTMC-KWx method seems best at lower energies. That the QTMC-KWx result is better than the QTMC-KW result here is probably fortuitous since the KWx modification was made to benefit one-electron processes.

All the quasiclassical methods are much too small for the double electron transfer. Presumably this failure is due to the importance of wave-function symmetry in this exactly resonant process. At higher energies ($\gtrsim$250 keV) the quasiclassical calculations of this double transfer appear to be much better, but the statistical uncertainty in the Monte Carlo makes this conclusion equivocal.

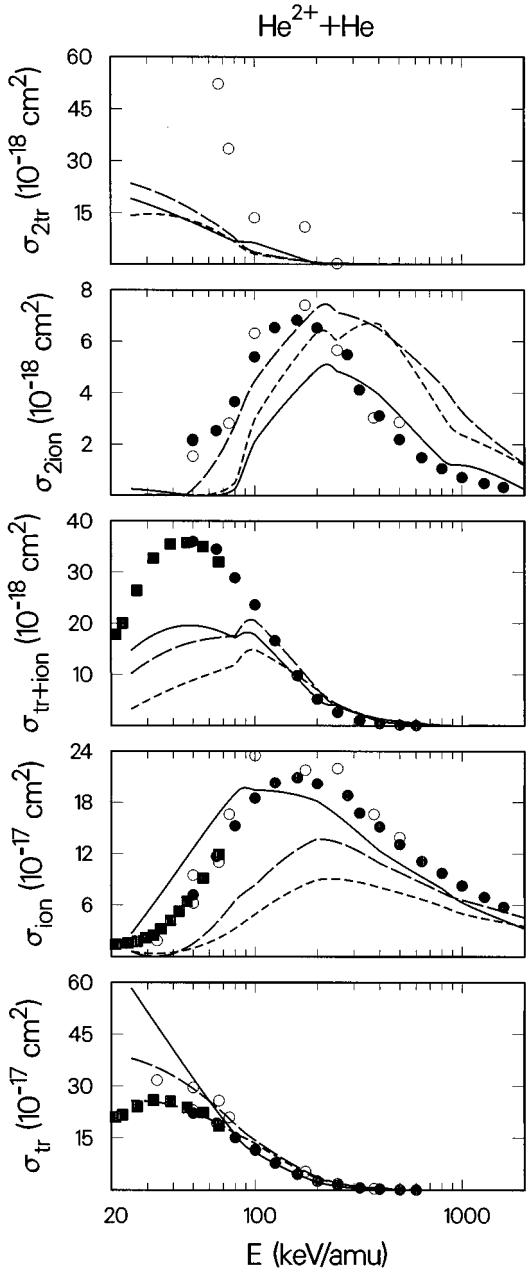

FIG. 10. Cross sections for He^{2+}+He collisions. Theoretical values are shown by curves: QTMC-KW (short dashed), QTMC-KWx (long dashed), QTMC-EB (solid). See the tables for the energies at which calculations were actually made and their statistical error bars. Experimental values are shown by data points: Shah and Gilbody [32] (filled circles), Shah, McCallion, and Gilbody [33] (filled squares), DuBois [34] (open circles).

Except for the symmetric double electron exchange, the quasiclassical results would certainly provide useful estimates in the absence of accurate experimental data.

E. Li^{3+}+He collisions

Cross sections for the two single-electron and three double-electron rearrangements possible in Li^{3+}+He collisions are shown in Fig. 11, and their error bars are indicated in Tables X–XIV. In these calculations, the initial internu-

TABLE V. Comparison of cross sections (in units of 10^{-17} cm^2) for the electron-transfer reaction $He^{2+}+He \rightarrow He^{+}+He^{+}$.

		$_{20}\sigma_{11}$(He,He)			
E (keV/amu)	v (a.u.)	Expt. [32]	QTMC-KW	QTMC-KWx	QTMC-EB
25.0	1.00		25.73±1.55	38.00±2.15	58.38±3.70
50.0	1.42	22.20±0.30	22.56±1.37	29.26±1.76	32.25±1.48
80.0	1.80	15.10±0.30	16.25±1.15	19.00±1.45	16.03±0.87
100.0	2.01	11.50±0.14	13.44±1.07	14.35±1.24	10.86±1.31
200.0	2.84	2.60±0.02	3.34±0.43	3.71±0.52	2.25±0.43
400.0	4.02	0.309±0.007	0.59±0.17	0.41±0.14	0.22±0.07

TABLE VI. Comparison of cross sections (in units of 10^{-17} cm^2) for the single-ionization reaction $He^{2+}+He \rightarrow He^{2+}+He^{+}+e$.

		$_{20}\sigma_{21}$(He,He)			
E (keV/amu)	v (a.u.)	Expt [32].	QTMC-KW	QTMC-KWx	QTMC-EB
25.0	1.00		0.59±0.34	0.59±0.34	2.67±0.99
50.0	1.42	7.20±0.31	0.99±0.44	1.54±0.58	12.60±1.15
80.0	1.80	15.25±0.26	3.29±0.72	6.53±1.06	19.00±1.10
100.0	2.01	18.50±0.21	4.94±0.84	8.36±1.16	19.42±1.81
200.0	2.84	20.20±0.30	8.97±0.65	13.72±0.92	18.13±1.09
400.0	4.02	15.14±0.21	8.06±0.59	10.88±0.60	12.33±0.45
800.0	5.68	9.74±0.14	5.89±0.31	7.49±0.39	7.96±0.40
1000.0	6.35	8.26±0.10	5.01±0.27	6.59±0.35	6.30±0.37
2000.0	8.98		3.54±0.25	4.53±0.27	3.27±0.27

TABLE VII. Comparison of cross sections (in units of 10^{-17} cm^2) for the transfer-ionization reaction $He^{2+}+He \rightarrow He^{+}+He^{2+}+e$.

		$_{20}\sigma_{12}$(He,He)			
E (keV/amu)	v (a.u.)	Expt [32].	QTMC-KW	QTMC-KWx	QTMC-EB
25.0	1.00		0.32±0.09	1.01±0.18	1.47±0.22
50.0	1.42	3.60±0.06	0.89±0.15	1.63±0.24	1.96±0.24
80.0	1.80	2.89±0.06	1.19±0.17	1.76±0.21	1.72±0.21
100.0	2.01	2.36±0.02	1.48±0.19	2.05±0.23	1.78±0.21
200.0	2.84	0.518±0.005	0.70±0.10	0.72±0.10	0.52±0.06
400.0	4.02	0.0427±0.0026	0.14±0.04	0.14±0.04	0.08±0.02

TABLE VIII. Comparison of cross sections (in units of 10^{-18} cm^2) for the double-ionization reaction $He^{2+}+He \rightarrow He^{2+}+He^{2+}+2e$.

		$_{20}\sigma_{22}$(He,He)			
E (keV/amu)	v (a.u.)	Expt. [32]	QTMC-KW	QTMC-KWx	QTMC-EB
80.0	1.80	3.66±0.41	0.49±0.35	2.72±1.01	0.25±0.25
100.0	2.01	5.40±0.34	2.97±0.91	4.45±1.14	2.10±0.74
200.0	2.84	6.53±0.21	6.35±0.91	7.30±0.96	4.90±0.67
400.0	4.02	3.11±0.11	6.68±0.97	6.49±1.02	4.00±0.48
800.0	5.68	1.053±0.047	3.20±0.45	4.33±0.51	1.41±0.30
1000.0	6.35	0.707±0.050	2.38±0.38	3.29±0.45	1.19±0.24
2000.0	8.98		1.19±0.24	1.24±0.24	0.25±0.11

TABLE IX. Comparison of cross sections (in units of 10^{-18} cm^2) for the double-transfer reaction $He^{2+}+He \rightarrow He+He^{2+}$.

		$_{20}\sigma_{02}$(He,He)			
E (keV/amu)	v (a.u.)	Expt. [34] [a]	QTMC-KW	QTMC-KWx	QTMC-EB
25.0	1.00		14.10±2.15	23.50±3.19	19.12±2.61
50.0	1.42	61.9, 76.8	12.62±1.86	15.83±2.14	12.13±1.83
80.0	1.80		6.43±1.27	7.67±1.55	6.65±1.39
100.0	2.01	13.5	2.97±0.84	3.46±0.97	6.19±1.33
200.0	2.84		0.54±0.27	0.51±0.26	0.19±0.12
250.0	3.17	0.169	0.31±0.12	0.31±0.12	0.13±0.08

[a]Uncertainly in experimental values is ±15%.

clear distance was $25a_0$ and the first range of impact parameters was [0,2] ([0,1] for the extra trajectories run for the double electron reactions).

Again the agreement with experiments is generally quite credible. The calculated double electron transfer cross sections here agree reasonably well with the experimental values, so we have some corroboration that the disagreement in the case of $He^{2+}+He \rightarrow He+He^{2+}$ is indeed due to the importance of wave-function symmetry there. As in the case of $He^{2+}+He$, the QTMC-KW(and KWx) cross sections for double ionization are considerably too large at the higher energies; the σ_{2ion} calculated by QTMC-KW seems to be shifted to higher energies relative to the experimental cross section. This deviation is somewhat disturbing since the quasiclassical description is expected to be valid at these energies. The QTMC-EB σ_{2ion} appears to be in much better agreement with the experimental determination.

IV. CONCLUSIONS

Two quasiclassical methods — the previously proposed QTMC-KW and the QTMC-EB approaches — have been shown to provide useful predictions of single and double electron rearrangements. The energy regime of validity is found to be similar to that of the usual CTMC method for one-electron systems. Even for one-electron systems some improvement may be obtained by eliminating transfer into orbitals more deeply bound than allowed by quantum mechanics. Quasiclassical approaches are most valid at collision velocities comparable to those of the target electrons, ~ 1 a.u., which is also where nonresonant electron-rearrangement cross sections tend to peak. At lower energies the quasiclassical approach tends to break down because of the importance of molecular structure effects on the evolution of the electron density during the collision. In the high-energy limit, where cross sections are generally too small to be amenable to a Monte Carlo approach anyway, the classical asymptotic dependence may not be quite correct; e.g., classically the single-ionization cross section falls off as $1/E$ instead of $(1/E)\log E$ [36]. The high-energy behavior of ionization is dominated by the perturbative contribution, which involves quantal tunneling.

The present applications were made to collisions of H^+, He^{2+}, and Li^{3+} with He, for which all the cross sections are generally well known experimentally. These comparisons provide guidance for future applications to other systems where cross sections are unknown. The only dramatic failure

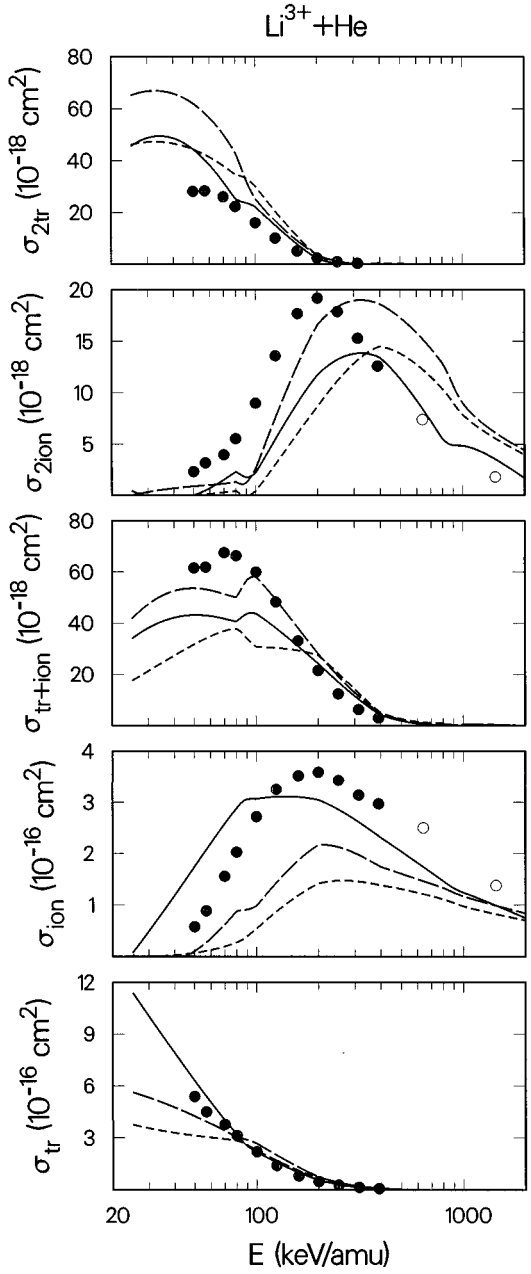

FIG. 11. Cross sections for $Li^{3+}+He$ collisions. Theoretical values are shown by curves: QTMC-KW (short dashed), QTMC-KWx (long dashed), QTMC-EB (solid). See the tables for the energies at which calculations were actually made and their statistical error bars. Experimental values are shown by data points: Shah and Gilbody [32] (filled circles), Knudsen *et al.* [35] (open circles).

TABLE X. Comparison of cross sections (in units of 10^{-16} cm^2) for the electron-transfer reaction $Li^{3+}+He \rightarrow Li^{2+}+He^{+}$.

		$_{30}\sigma_{21}$(Li,He)			
E (keV/amu)	v (a.u.)	Expt. [32]	QTMC-KW	QTMC-KWx	QTMC-EB
25.0	1.00		3.77±0.23	5.63±0.31	11.40±0.64
50.0	1.42	5.39±0.09	3.13±0.22	4.26±0.29	6.31±0.31
80.0	1.80	3.14±0.03	2.83±0.21	3.05±0.25	2.79±0.31
100.0	2.01	2.20±0.02	2.28±0.19	2.67±0.23	2.36±0.27
200.0	2.84	0.479±0.004	0.65±0.08	0.74±0.12	0.56±0.10
400.0	4.02		0.10±0.03	0.07±0.03	0.06±0.03

TABLE XI. Comparison of cross sections (in units of 10^{-16} cm^2) for the single-ionization reaction $Li^{3+}+He \rightarrow Li^{3+}+He^{+}+e$.

		$_{30}\sigma_{31}$(Li,He)			
E (keV/amu)	v (a.u.)	Expt. [32]	QTMC-KW	QTMC-KWx	QTMC-EB
25.0	1.00		$\lesssim$0.02	0.04±0.04	0.07±0.05
50.0	1.42	0.58±0.06	0.07±0.05	0.11±0.08	1.74±0.24
80.0	1.80	2.03±0.07	0.28±0.09	0.88±0.18	2.88±0.18
100.0	2.01	2.72±0.12	0.54±0.12	0.99±0.18	3.06±0.28
200.0	2.84	3.59±0.12	1.42±0.12	2.17±0.18	3.05±0.21
400.0	4.02		1.38±0.10	1.74±0.10	2.31±0.13
800.0	5.68		1.11±0.06	1.33±0.07	1.47±0.08
1000.0	6.35		0.97±0.05	1.17±0.06	1.24±0.07
2000.0	8.98		0.70±0.05	0.84±0.05	0.75±0.05

TABLE XII. Comparison of cross sections (in units of 10^{-17} cm^2) for the transfer-ionization reaction $Li^{3+}+He \rightarrow Li^{2+}+He^{+}+e$.

		$_{30}\sigma_{21}$(Li,He)			
E (keV/amu)	v (a.u.)	Expt. [32]	QTMC-KW	QTMC-KWx	QTMC-EB
25.0	1.00		1.76±0.29	4.18±0.51	3.40±0.40
50.0	1.42	6.16±0.13	3.17±0.38	5.37±0.55	4.32±0.44
80.0	1.80	6.64±0.10	3.78±0.40	5.01±0.47	4.07±0.25
100.0	2.01	6.00±0.11	3.08±0.36	5.81±0.50	4.37±0.28
200.0	2.84	2.15±0.04	2.74±0.23	2.81±0.23	2.43±0.23
400.0	4.02		0.51±0.10	0.48±0.10	0.42±0.09
800.0	5.68		0.10±0.03	0.07±0.02	0.03±0.02

TABLE XIII. Comparison of cross sections (in units of 10^{-18} cm^2) for the double-ionization reaction $Li^{3+}+He \rightarrow Li^{3+}+He^{2+}+2e$.

		$_{30}\sigma_{32}$(Li,He)			
E (keV/amu)	v (a.u.)	Expt. [32]	QTMC-KW	QTMC-KWx	QTMC-EB
80.0	1.80	5.54±0.31	0.44±0.44	1.32±0.98	2.30±0.63
100.0	2.01	9.00±0.60	0.44±0.44	2.64±1.24	2.21±0.88
200.0	2.84	19.20±0.80	8.65±1.36	16.61±1.92	11.74±1.58
400.0	4.02		14.51±1.98	18.61±2.31	13.43±1.82
800.0	5.68		10.38±1.05	12.88±1.21	5.54±0.74
1000.0	6.35		7.92±0.86	9.06±0.95	4.84±0.71
2000.0	8.98		3.96±0.58	4.40±0.61	1.67±0.38

TABLE XIV. Comparison of cross sections (in units of 10^{-17} cm^2) for the double-transfer reaction $Li^{3+}+He \rightarrow Li^{+}+He^{2+}$.

		$_{30}\sigma_{12}$(Li,He)			
E (keV/amu)	v (a.u.)	Expt. [32]	QTMC-KW	QTMC-KWx	QTMC-EB
25.0	1.00		4.62±0.46	6.51±0.63	4.56±0.47
50.0	1.42	2.82±0.04	4.44±0.40	6.20±0.54	4.45±0.41
80.0	1.80	2.24±0.04	3.48±0.35	4.31±0.43	2.54±0.20
100.0	2.01	1.60±0.03	3.03±0.32	2.55±0.32	2.25±0.21
200.0	2.84	0.231±0.015	0.33±0.09	0.35±0.09	0.21±0.07

was for resonant double electron transfer in $He^{2+}+He$ collisions where wave-function symmetry is expected to play an essential role.

The two great selling points of the QTMC methods are (i) their ease of use and (ii) the consistent and simultaneous treatments of all electron rearrangements. The regime of greatest utility is expected to be at intermediate energies where all the processes tend to have significant cross sections, electronic continua are important, and quantum-mechanical basis-set methods are slowly convergent. The methods are intended as simple tools for understanding and visualizing dynamic mechanisms as well as for calculating useful cross sections, but not as vehicles for high-precision tests. The methods can lend some qualitative guidance for, but certainly will not supplant, quantum-mechanical developments.

Quasiclassical methods employed in the past (mentioned in Sec. I) for helium targets, which achieved stability by considering one-electron subsystems or neglecting electron correlation [10,11,13,16], also obtained fairly accurate cross sections for single charge transfer and single ionization at $E \gtrsim 100$ keV/amu. A method that achieved limited stability via circular orbits for the electrons [14] is in agreement at $E \gtrsim 1000$ keV/amu. Only the paper of Wetmore and Olson [16], which neglected the electron-electron force, gave detailed results for the two-electron processes ($\sigma_{\mathrm{tr+ion}}$, σ_{2ion}, and σ_{2tr}). Their results for $\sigma_{\mathrm{tr+ion}}$ are comparable with the present results in the cases of He^{2+} and Li^{3+} projectiles but are much too small for the H^{+} projectile (as are the KW and KWx results in the present work). Their results for σ_{2ion} are not as good. Their results for σ_{2tr} are very good for Li^{3+}, and are not given for He^{2+} for which no classical method is expected to be valid. Other than accuracy considerations, an advantage of the present methods over these earlier approaches are their generality in treating the full interactions of all electrons.

The QTMC-EB method gives more accurate cross sections than the QTMC-KW method in most cases, but this improvement has been bought with a price. QTMC-EB is not as ''*ab initio*'' as QTMC-KW. It cannot predict atomic binding energies like the KW approach. On the other hand, there is some advantage to this less-ambitious approach in that the binding energies can be specified *ad hoc*. Atomic binding energies are accurately known from quantum-mechanical calculations, and it is the collisional dynamics with these targets that sometimes still remains perplexing. Some improvement in the QTMC-KW cross sections was obtained by a modification, designated QTMC-KWx, in which the ξ parameter was adjusted to give the quasiclassical helium atom its accurate ionization potential.

Another advantage of the QTMC-EB approach is that the target is dynamic; i.e., the ground-state electrons have velocity and not just momentum as in the QTMC-KW description. Velocity matching was expected to be important in some electron-transfer processes. However, the results seem to indicate that the KW effective momentum generally provides an adequate description even though it is not simply related to a velocity. In any event, this feature is not of great concern to ionizing processes, where QTMC-KW has already proved to be useful [21,22].

The full advantage of the EB flexibility was not required in the present calculations on the helium atom since for this atom there are only two electrons in the same subshell. In general, the EB approach would allow each subshell to be assigned its own energy bound; again there would be a price to be paid — here loss of fully identical treatment of all electrons. Further development of the EB approach is needed for the general many-electron situation. The present stage of development seems to extend the proved utility of the CTMC method to at least two-electron targets.

[1] R. Abrines and I. C. Percival, Proc. Phys. Soc. London **88**, 861 (1966).

[2] R. E. Olson and J. Wang, in *The Physics of Electronic and Atomic Collisions, XVIII International Conference*, edited by T. Andersen *et al.*, AIP Conference Proceedings No. 295 (AIP, New York, 1993), pp. 520–533.

[3] J. S. Cohen, Phys. Rev. A **27**, 167 (1983).

[4] Comput. Phys. Commun. **63**, (1991), special issue on time-dependent methods for quantum dynamics, edited by K. C. Kulander.

[5] H. Kröger, Phys. Rep. **210**, 45 (1992).

[6] J. D. Garcia, N. H. Kwong, and J. S. Cohen, Phys. Rev. A **35**, 4068 (1987).

[7] N. H. Kwong, J. D. Garcia, and J. S. Cohen, J. Phys. B **22**,

L633 (1989).
[8] V. Vesovic, W. A. Wakeham, A. S. Dickinson, F. R. W. McCourt, and M. Thachuk, Mol. Phys. **84**, 553 (1995).
[9] I. C. Percival and D. Richards, Adv. At. Mol. Phys. **11**, 1 (1975).
[10] R. E. Olson, Phys. Rev. A **18**, 2464 (1978).
[11] G. Peach, S. L. Willis, and M. R. C. McDowell, J. Phys. B **18**, 3921 (1985); S. L. Willis, G. Peach, M. R. C. McDowell, and J. Banerji, *ibid.* **18**, 3939 (1985).
[12] J. H. McGuire and L. Weaver, Phys. Rev. A **16**, 41 (1977).
[13] R. E. Olson, in *Electronic and Atomic Collisions*, Invited papers of the XV International Conference on the Physics of Electronic and Atomic Collisions, edited by H. B. Gilbody *et al.* (North-Holland, Amsterdam, 1988), pp. 271–285.
[14] M. L. McKenzie and R. E. Olson, Phys. Rev. A **35**, 2863 (1987).
[15] J. S. Cohen, Phys. Rev. A **36**, 2024 (1987).
[16] A. E. Wetmore and R. E. Olson, Phys. Rev. A **38**, 5563 (1988).
[17] C. L. Kirschbaum and L. Wilets, Phys. Rev. A **21**, 834 (1980).
[18] J. S. Cohen, Phys. Rev. A **51**, 266 (1995).
[19] J. S. Briggs and J. H. Macek, Adv. At. Mol. Opt. Phys. **28**, 1 (1990).
[20] D. Zajfman and D. Maor, Phys. Rev. Lett. **56**, 320 (1986).
[21] D. A. Wasson and S. E. Koonin, Phys. Rev. A **39**, 5676 (1989).
[22] P. B. Lerner, K. J. LaGattuta, and J. S. Cohen, Laser Phys. **3**, 331 (1993); Phys. Rev. A **49**, R12 (1994).
[23] W. A. Beck, L. Wilets, and M. A. Alberg, Phys. Rev. A **48**, 2779 (1993).
[24] J. S. Cohen, Phys. Rev. A **26**, 3008 (1982).
[25] L. Wilets, E. M. Henley, M. Kraft, and A. D. MacKellar, Nucl. Phys. A **282**, 341 (1977).
[26] J. S. Cohen, J. Phys. B **18**, 1759 (1985).
[27] G. W. Kerby, M. W. Gealy, Y.-Y. Hsu, M. E. Rudd, D. R. Schultz, and C. O. Reinhold, Phys. Rev. A **51**, 2256 (1995).
[28] R. E. Olson, Phys. Rev. A **24**, 1726 (1981).
[29] M. B. Shah and H. B. Gilbody, J. Phys. B **14**, 2361 (1981).
[30] M. B. Shah, D. S. Elliott, and H. B. Gilbody, J. Phys. B **20**, 2481 (1987).
[31] G. W. McClure, Phys. Rev. **148**, 47 (1966).
[32] M. B. Shah and H. B. Gilbody, J. Phys. B **18**, 899 (1985).
[33] M. B. Shah, P. McCallion, and H. B. Gilbody, J. Phys. B **22**, 3037 (1989).
[34] R. D. DuBois, Phys. Rev. A **36**, 2585 (1987).
[35] H. Knudsen *et al.*, J. Phys. B **17**, 3545 (1984).
[36] D. R. Bates, Phys. Rep. **35**, 305 (1978).